Available online at www.sciencedirect.com
SCIENCE DIRECT
Polymer 47 (2006) 4781–4788
polymer
www.elsevier.com/locate/polymer

Enthalpy recovery of polymeric glasses: Is the theoretical limiting liquid line reached?

Qingxiu Li, Sindee L. Simon *

Department of Chemical Engineering, Texas Tech University, Lubbock, TX 79409, USA

Received 16 December 2005; received in revised form 19 April 2006; accepted 20 April 2006
Available online 18 May 2006

Abstract

Glasses are inherently non-equilibrium materials, and consequently, their properties evolve toward equilibrium in a process known as structural recovery or physical aging. Recently, several authors have suggested that the equilibrium liquid line is not reached even when properties have ceased to evolve. In this work, we present measurements of the enthalpy recovery of polystyrene (PS) at temperatures ranging from 90.0 to 103.0 °C, for aging times up to 200 days. The results are analyzed in the context of the TNM model of structural recovery. In addition, we analyze data in the literature to determine whether enthalpy recovery ceases prior to the material reaching the equilibrium liquid line obtained by extrapolation of the liquid line above T_g. The results suggest that, in fact, the liquid enthalpy line is reached at temperatures below T_g when equilibrium is reached, i.e. when properties cease to evolve.

Keywords: Enthalpy recovery; Polystyrene; TNM/KAHR model

1. Introduction

Glassy materials are characterized by their thermodynamic non-equilibrium nature; as a result, the physical and mechanical properties of these materials evolve toward the equilibrium state. This behavior is termed structural recovery or physical aging in the literature, with structural recovery generally referring to evolution of volume and enthalpy, and physical aging generally referring to changes in mechanical properties. Several reviews have been written [1–4]. A fundamental understanding of structural recovery and physical aging is important for predicting the long-term performance of these materials.

The Kovacs–Aklonis–Hutchinson–Ramos (KAHR) model [5] and the Tool–Narayanaswamy–Moynihan (TNM) model [6–8] of structural recovery are equivalent multi-parameter phenomenological models, which describe the phenomenology associated with the glass transition, including the non-linearity and non-exponentiality of structural recovery. Although the TNM/KAHR model is known to be inadequate for describing behavior over a wide range of thermal histories due to the dependence of the model parameters on thermal history [1–3,9–17] arising, perhaps, from a dependence of the relaxation time on thermal history [18], the model is able to describe, for example, structural recovery after down jumps over a limited temperature range. An implicit assumption in the TNM/KAHR model is that the structural recovery of glassy materials proceeds until the material reaches its theoretical limit, the extrapolated liquid line. According to Hutchinson and Kumar [19], Kovacs [20] demonstrated that volume recovery proceeds to the extrapolated liquid line, but in most dilatometric studies, whether or not the volume at equilibrium (v_∞) corresponds to the expected liquid line is not explicitly stated. Similarly, in calorimetric studies, including adiabatic calorimetry [21–23], whether or not the enthalpy at equilibrium corresponds to the expected liquid line is not explicitly stated.

For the case of enthalpy recovery, whether the enthalpy at equilibrium corresponds to the expected liquid line cannot be explicitly measured since enthalpy is not an absolute quantity. However, one can determine whether the enthalpy loss at equilibrium ($\Delta H_{a\infty}$) corresponds to that expected if the liquid line is reached. The value of $\Delta H_{a\infty}$ for a perfect quench from T_0 to an aging temperature (T_a) below T_g equals the product of ΔC_p and the difference between the initial fictive temperature ($=T_0$ for a perfect quench) and the aging temperature

$$\Delta H_{a\infty} = \Delta C_p(T_0 - T_a) \tag{1}$$

* Corresponding author. Tel.: +1 806 742 1763; fax: +1 806 742 3552.
E-mail address: sindee.simon@ttu.edu (S.L. Simon).

0032-3861/$ - see front matter © 2006 Elsevier Ltd. All rights reserved.
doi:10.1016/j.polymer.2006.04.046

where ΔC_p is the step change in the heat capacity at glass transition temperature. Based on this equation, the slope $-d\Delta H_{a\infty}/dT_a$ is expected to be equivalent to ΔC_p. However, due to the breadth of the glass transition region and for finite cooling rates, $\Delta H_{a\infty}$ will be lower than predicted by this expression for aging temperatures near T_g. Consequently, the value of $-d\Delta H_{a\infty}/dT_a$ obtained from enthalpy relaxation data may be lower than the value of ΔC_p. This observation has, in fact, often been misinterpreted with researchers suggesting that the liquid enthalpy line is not reached at equilibrium [24–26].

Moreover, based on the fact that $-d\Delta H_{a\infty}/dT_a$ was less than ΔC_p, Cowie and co-workers took $\Delta H_{a\infty}$ to be a fitting parameter in their model of structural relaxation [24–26]. They fit their enthalpy relaxation data using a stretched exponential (KWW) function

$$\delta_h = \Delta H_{a\infty} - \Delta H_a(t) = \delta_{h0}\exp\left\{-\left(\frac{t}{\tau_0}\right)^{\beta}\right\} \quad (2)$$

where $\Delta H_a(t)$ is the enthalpy loss at aging time t, δ_{h0} is the initial enthalpic departure from the equilibrium, τ_0 is the characteristic relaxation time, and β is the non-exponentiality parameter in the Kohlrausch–William–Watts (KWW) function [27,28]. In addition to allowing $\Delta H_{a\infty}$ to be a fitting parameter, the characteristic relaxation time τ_0 in the Cowie–Ferguson model is a constant in contrast to the TNM/KAHR approach. As a result, Eq. (2) fails to account for the non-linearity of the relaxation process and cannot readily describe asymmetry of approach data [3,5].

In spite of the shortcomings of the Cowie–Ferguson model, Cowie and coworkers fit enthalpy relaxation data, which had not reached equilibrium using their model and obtained values of $\Delta H_{a\infty}$ significantly lower than those predicted from the extrapolation of liquid line [24–26]. Hutchinson and Kumar [19] have correctly argued that Cowie's underestimation of $\Delta H_{a\infty}$ arises from their omission of the non-linearity of the process. However, the postulate put forth by Cowie and coworkers that the theoretical enthalpy limit is not achievable promoted the development of a configurational entropy model by Gómez-Ribelles et al. [29–31], in which the relaxation time is a function of temperature and configurational entropy S_c, and the equilibrium configurational entropy is assumed to be higher than the limiting configurational entropy from the extrapolated liquid line [29–31]. Gómez-Ribelles and coworkers determined the heat capacity difference between the so-called equilibrium state and the extrapolation from the liquid line, δ, upon curve fitting isothermal aging data to the configurational entropy model. However, the isothermal aging data in their experiments did not reached the actual equilibrium state; as a result, even though the model can describe the experimental data for short aging times, it does not necessarily predict the correct long-time equilibrium data. In addition to the Cowie–Ferguson and the Gómez-Ribelles models, Colby's scaling model [32] also implies that there exists a critical temperature, T_c, below which the theoretical enthalpy limit is not achieved; this temperature is said to be approximately 10 °C below T_g for polymers.

In this paper, we address whether the theoretical enthalpy limit is reached during enthalpy relaxation. New measurements are carried out for polystyrene at temperatures ranging from the vicinity of glass transition temperature to 90 °C, approximately 10 °C below the nominal T_g, for up to 200 days. In addition, the enthalpy relaxation data on other polymers and small molecule glass formers in the literature is re-examined for cases where equilibrium was achieved at multiple aging temperatures in an effort to generalize our conclusion that the liquid line is reached when equilibrium is achieved (i.e. when enthalpy stops evolving).

1.1. TNM model

The TNM model describes the evolution of the enthalpic departure from the equilibrium, δ_h, during isothermal aging after a temperature jump from equilibrium as follows

$$\delta_h = \Delta H_{a\infty} - \Delta H_a(t) = \delta_{h0}\exp\left\{-\left(\int_0^t \frac{dt}{\tau_0}\right)^{\beta}\right\} \quad (3)$$

where $\Delta H_{a\infty}$ is the equilibrium enthalpy loss at the aging temperature, $\Delta H_a(t)$ is the enthalpy loss at aging time t, δ_{h0} is the initial enthalpic departure from the equilibrium, τ_0 is the characteristic relaxation time, and β is the non-exponentiality parameter in the Kohlrausch–William–Watts (KWW) function [27,28]. The characteristic relaxation time τ_0 is a function of temperature and the departure from equilibrium, the latter of which accounts for the non-linearity of structural relaxation [5,6,8]:

$$\ln \tau_0 = \ln A + \frac{\Delta h}{RT} + \frac{(1-x)\Delta h}{RT_f} \quad (4)$$

where $\ln A$ is the pre-exponential factor, Δh is the apparent activation energy, x is the non-linearity parameter, and T_f is the fictive temperature, which is related to δ_h by

$$T_f = T_a + \frac{\delta_h}{\Delta C_p} \quad (5)$$

Eq. (4) is based on the TNM formalism. Eq. (3) assumes a perfect quench when jumping to the aging temperature. For multi-step thermal histories or finite temperature ramps, Boltzmann superposition [33] is applied [5,8]. For the narrow temperature investigated and at temperatures below the nominal T_g of the material, the Arrhenius temperature dependence of the equilibrium relaxation time (when $T_f = T$) assumed in Eq. (4) has been shown to be valid [34]; i.e. the equilibrium relaxation time is found to not follow the expected WLF/VTHF [35–38] temperature dependence below the nominal T_g. This assumption is also verified by data presented later in this work.

2. Methodology

2.1. Materials

The polymer used in this study is polystyrene, Dylene 8 from Arco Polymers, with a number-average molecular weight of 92,800 g/mol, a weight-average molecular weight of 221,000 g/mol, and a z-average molecular weight of 423,000 g/mol. This polystyrene is identical to that used in the earlier study by Simon et al. [34].

2.2. DSC measurements

A Perkin–Elmer Pyris 1 differential scanning calorimeter (DSC) with an ethylene glycol cooling system set to 5 °C was used for enthalpy recovery measurements at aging temperatures ranging from 90 to 103 °C and for measurement of the dependence of limiting fictive temperature, T_f', on cooling rate for cooling rates ranging from 0.01 to 30 K/min. For aging studies, the sample was held at 130 °C in the DSC for 3 min to erase its thermal history and was subsequently quenched to the aging temperature at 30 K/min. For aging treatments ranging from 5 min to 24 h, aging was carried out in the DSC itself using a single sample of 10.74 mg for all runs. Each aging experiment was repeated three times. After aging for a specified time, the sample was quenched from the aging temperature to 40 °C at 30 K/min and then heated to 130 °C at 10 K/min to collect the aged scan. After the aged scan, an unaged scan was collected by quenching the sample directly from 130 to 40 °C at 30 K/min and then the unaged scan was immediately run by heating to 130 °C at 10 K/min. The enthalpy loss (ΔH_a) during the aging process was determined by the difference in the areas under the aged and unaged scans [39]. Since the unaged scans were those collected immediately after the corresponding aged scans, the error introduced by instrument baseline drift is minimized. We note that the highest cooling rate in this study, 30 K/min, is realized down to 80 °C with an ethylene glycol cooler set to 5 °C, which is sufficient to cover the glass transition region of polystyrene at this cooling rate.

Since the time required to reach equilibrium at 90.0 °C is on the order of weeks, aging at this temperature was also performed outside the DSC in a Fisher Isotemp® oven after an initial pretreatment in the DSC of holding the sample at 130 °C for 3 min and then quenching it to 90.0 °C at 30 K/min. Three replicates were measured at each aging time ranging from 2 h to 200 days for oven-aged samples. In addition, to ensure that systematic temperature variations did not influence the results, additional samples were put in the oven at day 23 and aged for 1, 2, 7, 14, and 21 days with three replicate samples again used for each aging time. Oven-aged samples with weights of 10.40 ± 0.58 mg were placed in a heavy steel box with flowing dry nitrogen. The sample temperature in the oven was monitored by an Omega DP460 temperature indicator, which was calibrated with a 1560 Black Stack from Hart Scientific. The sample temperature variation was ± 0.6 °C over 5 days. After aging for a specified time, the samples were removed from the oven and placed in the DSC furnace at 90.0 °C; the samples were held at 90.0 °C for 3 min and then quenched to 40 °C at 30 K/min. Aged and unaged scans were performed to determine enthalpy loss as described above. The data obtained from the samples aged at 90.0 °C in the DSC and in the oven at the overlapping aging times of 2, 4, 8, and 24 h were comparable (as shown in the results) indicating that all aging treatments were equivalent.

The effect of cooling rate (q_c) on the limiting fictive temperature (T_f') was determined using a single sample of 9.68 mg. The sample was held at 130 °C for 3 min and cooled to 50 °C at a specified rate, and subsequently heated to 140 °C at a rate of 10 K/min; at the end of the run, the sample temperature was reduced to 50 °C. (Note that heating to 140 °C was necessary to ensure observation of the full enthalpic relaxation peak for the slowest cooling rates). For the slowest cooling rates of 0.01 and 0.03 K/min, the specified cooling rates were applied only in the expected glass transition range from 101 to 85 °C and from 110 to 70 °C, respectively; a 1 K/min was applied in the remainder of the temperature range from 130 to 50 °C in order to reduce run time. Each experiment was repeated three times. The limiting fictive temperature T_f' was determined by the method proposed by Moynihan et al. [8,40,41]

$$\int_{T_f'}^{T \gg T_g} (C_{pl} - C_{pg}) dT = \int_{T \ll T_g}^{T \gg T_g} (C_p - C_{pg}) dT \quad (6)$$

where C_{pl} and C_{pg} are the liquid and glass heat capacities, respectively, and C_p is the apparent heat capacity of the material measured by DSC. Accordingly, the heat flow of the DSC curve was integrated and the limiting fictive temperature was determined by the interception of the extrapolation of the liquid enthalpy line and the glassy enthalpy line. The standard error of the limiting fictive temperature was within ± 0.2 °C for the three replicate runs.

The temperature and heat flow of the DSC were calibrated with a liquid crystal standard (+)-4-*n*-hexyloxyphenyl-4′-(2′-methylbutyl)-biphenyl-4-carboxylate (CE-3) and with indium at a heating rate of 10 K/min. Following the calibration, the isothermal temperature of the DSC was corrected by the difference of the melting point of indium at 0.1 K/min and that at 10 K/min [42]. The temperature calibration of the DSC was maintained within ± 0.1 °C, and it was checked with indium at regular intervals. The standard errors in the enthalpy loss for polystyrene aged at all temperatures in the DSC and in the oven are within ± 0.05 and ± 0.15 J/g, respectively; the error from the DSC data is less than that previously reported by Simon et al. [34].

2.3. Model calculations

The Tool–Narayanaswamy–Moynihan (TNM) model was used to fit the enthalpy recovery data measured in the current study and that obtained in our earlier study [34].

The computer program used to determine the TNM model parameters was SRS602 written in Visual Basic 6.0 by Sobieski [42]. An imperfect quench was applied for modeling the enthalpy relaxation data by including a cooling ramp from 130 °C to the aging temperature at 30 K/min followed by the isothermal aging. The Marquardt algorithm was used during the parameter search [43]. The apparent activation energy $\Delta h/R$ was fixed; its value was determined based on the cooling rate dependence of the limiting fictive temperature and the aging temperature dependence of the time required to reach equilibrium. The other three parameters, the non-linearity parameter x, the non-exponentiality parameter β, and the pre-exponential factor ln A, in the model were then determined by the curve fitting procedure. The ΔC_p used in the model (0.265 J/g/K) was determined from the cooling run at 30 K/min in the DSC measurements. We not that in our previous work [34], we reported a ΔC_p of 0.25 J/g/K consistent with what is used here. However, in our previous work we also used ΔC_p of 0.22 J/g/K in the modeling because we assumed a prefect quench and that $-d\Delta H_{a\infty}/dT = \Delta C_p$.

3. Results and discussion

3.1. Enthalpy loss as a function of aging time for polystyrene

Fig. 1 shows the enthalpy loss as a function of aging time for polystyrene at temperatures ranging from 88.0 to 103.0 °C. The data at 90.0, 95.6, 99.0, 100.0, and 103.0 °C are from the current study, and the data at other aging temperatures are from our earlier study [34]. The enthalpy loss data at 95.6 °C obtained from the present study and from our earlier study are plotted in different symbols and show comparable behavior, indicating the experimental consistency of the two studies. The enthalpy loss increases linearly with aging time at a rate of approximately 0.6 J/g per logarithmic decade of time and levels off when equilibrium is reached. The time required to reach equilibrium (t_∞), as well as the equilibrium enthalpy loss ($\Delta H_{a\infty}$), increases with decreasing aging temperature. At the lowest aging temperature at which the equilibrium was achieved, 90.0 °C, the enthalpy loss levels off at an aging time of approximately 28 days [$\log(t_a/s) = 6.4$]. The enthalpy loss data for the samples aged at 90.0 °C in the DSC and in the oven are plotted in different symbols, as are the samples put in the oven at day 23. No discrepancy is observed between the different aging treatments although the data for the oven-aged samples do show more scatter because the temperature stability in the oven (±0.6 °C over 5 days) is considerably lower than that in the DSC. However, neither the time required to reach equilibrium nor the logarithmic aging rate are sensitive to these fluctuations, presumably because the relaxation time at equilibrium and the time required to reach equilibrium are orders of magnitude larger than the time scale for temperature variation in the oven.

The dependence of the enthalpy loss at equilibrium ($\Delta H_{a\infty}$) on aging temperature for the data shown in Fig. 1 is shown in Fig. 2 for temperatures where equilibrium was reached within the scatter of the data (i.e. for all aging temperatures except 91.0 and 88.0 °C); $\Delta H_{a\infty}$ is calculated by averaging the values after the enthalpy change has leveled off. The TNM model successfully predicts the dependence of $\Delta H_{a\infty}$ on T_a for a cooling ramp of 30 K/min from 130 °C as shown by the solid line; the model parameters are listed in Table 1. The dashed line shows the slope of 0.265 J/g/K, the value of ΔC_p on cooling. The data and the model show a transition region with a width of about 20 K, below which the slope of $\Delta H_{a\infty}$ versus

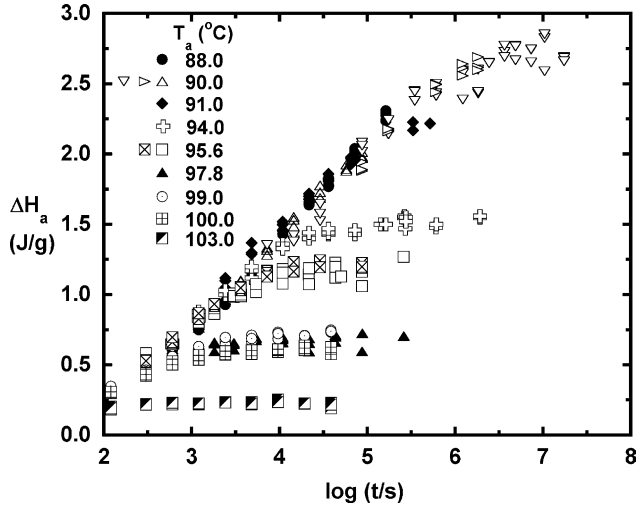

Fig. 1. Enthalpy loss as a function of aging time for polystyrene. Symbols are shown in the legend. For the aging data at 90.0 °C, ▽ shows the data aged in the oven, ▷ shows the data from the oven check run starting from day 23, and △ shows the aging data in the DSC. For the aging data at 95.6 °C, ⊠ shows the data from the current study and □ shows the data from our earlier study [34]. In addition, the data at 88.0, 91.0, 94.0, 95.6, and 97.8 °C are from the earlier study by Simon et al. [34].

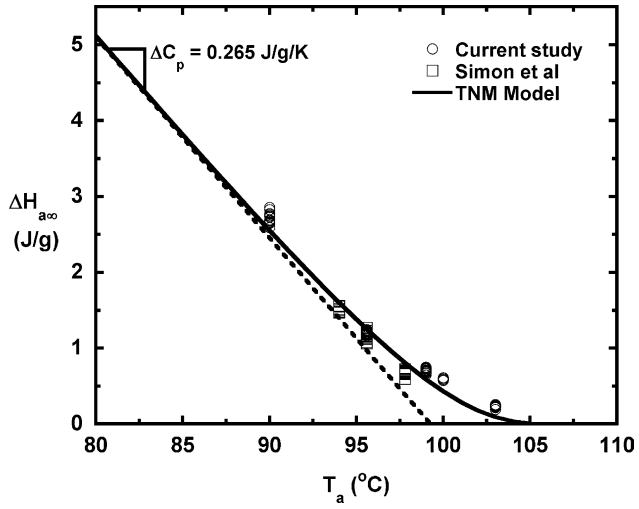

Fig. 2. Equilibrium enthalpy loss as a function of aging temperature for polystyrene. The data obtained from the current study is shown as ○ and the data from the earlier study by Simon et al. [34] is shown as □. The two sets of data overlap at $T_a = 95.6$ °C. The solid line shows the TNM model fit, and the dashed line shows a ΔC_p of 0.265 J/g/K and a T_{fo} of 99.3 °C.

Table 1
The TNM model parameters used to model the enthalpy relaxation data in the current study and those reported by Simon et al. [34]

Parameters	Enthalpy relaxation	
	Current study—imperfect quench	Simon et al.—perfect quench
$\Delta h/R$ (kK)	126.6	100.4
β	0.53	0.74
x	0.37	0.36
log τ_∞ at T_g=97 °C (s)	2.69	3.03
ln (A/s)	−335.83	−264.25
T_{fo} (°C)	N/A[a]	100.7
ΔC_p (J/g/K)	0.265	0.22[b]

[a] N/A, not applicable.
[b] The value of ΔC_p used in the model in Ref. [34] was not the experimental value; rather, in that work, we assumed $\Delta C_p = -d\Delta H_{a\infty}/dT$.

T_a is equivalent to ΔC_p. For experiments conducted at higher aging temperatures, which are necessary for achieving equilibrium in a reasonable time scale, the slope of $\Delta H_{a\infty}$ versus T_a is expected to be less than ΔC_p, not because aging does not progress to the theoretical liquid line as suggested by Cowie et al. [24–26], but because of the breadth of the transition region. Our result is consistent with one of the arguments put forward by Hutchinson and Kumar [19] for why $\Delta H_{a\infty} \neq \Delta C_p \Delta T$, although we show here that the breadth of the glass transition region can by itself satisfactorily explain the dependence of $\Delta H_{a\infty}$ on temperature. The issue of the temperature dependence of the heat capacities raised in Ref. [19], which we neglected, is anticipated to become more important as the temperature range of measurements is extended.

The data in Fig. 1 are transformed to δ_h ($=\Delta H_{a\infty} - \Delta H_a$) and are plotted in Fig. 3 with only the average of repeat runs shown. The fit of the TNM model to the experimental data is shown as solid lines in the figure; the model parameters are the same as those used to fit the $\Delta H_{a\infty}$ versus T_a data shown in

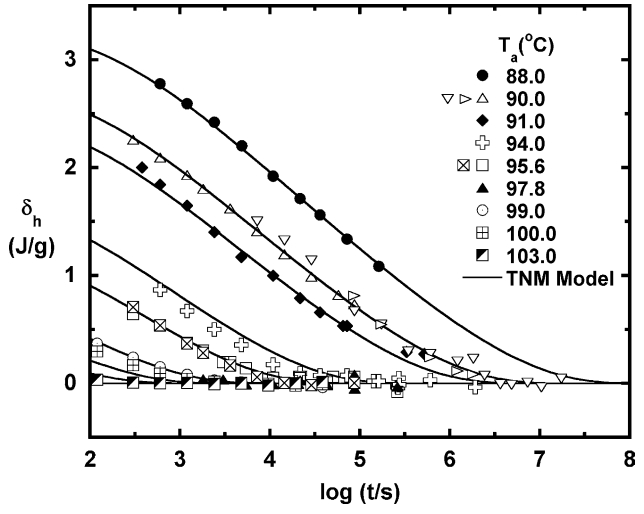

Fig. 3. Enthalpic departure from the equilibrium as a function of aging time for polystyrene for the data in Fig. 1 showing the average of repeat runs. Symbols are the same as in the caption for Fig. 1.

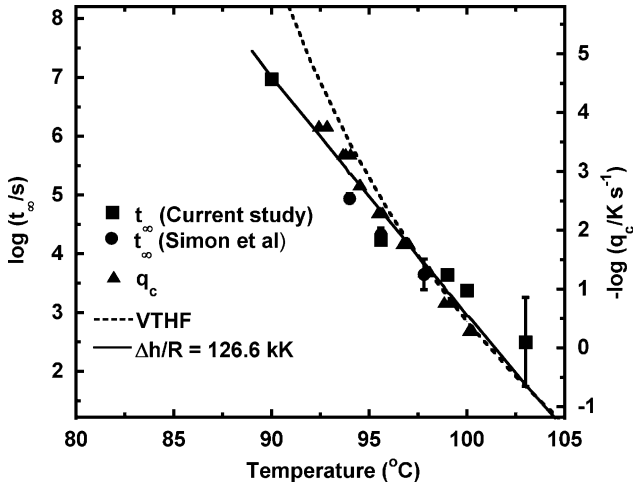

Fig. 4. Logarithmic time required to reach equilibrium as a function of aging temperature, with ■ showing the data from the current study and ● showing the data from the earlier study by Simon et al. [34], as well as the logarithmic cooling rate versus the limiting fictive temperature shown as ▲. The solid line represents the fit with $\Delta h/R$=126.6 K, and the dashed line represents the VTHF equation [34]: $\log t_\infty/t_{\infty,ref} = -12.8 + 370/(T - T_\infty)$, where T_∞=69.8 °C, T_{ref}=98.7 °C, and $t_{\infty,ref}$=2512 s.

Fig. 2, and a cooling rate of 30 K/min from 130 °C was used for modeling both sets of data. We note that in our previous work we assumed a perfect quench in our model calculations; as a result, the parameters for $\Delta h/R$, β, and ln A differ significantly as indicated in Table 1. This finding is consistent with the results [42] from model fits to volume data for imperfect and perfect quenches.

The time required to reach equilibrium (t_∞) as a function of aging temperature is plotted in Fig. 4 along with our earlier data [34]. The time required to reach equilibrium was determined by fitting the enthalpy loss data near equilibrium to the KWW function for each aging temperature and calculating the time required to reach δ_h=0.01 J/g [34]. Also plotted in Fig. 4 is the dependence of limiting fictive temperature T_f' on the cooling rate obtained from both the experiments and the TNM modeling. The cooling rate dependence of the limiting fictive temperature and the aging temperature dependence of the time required to reach equilibrium are both expected to follow the same trends, and to provide the apparent activation energy Δh [8,41]:

$$\frac{\Delta h}{R} = -\frac{d \ln|q_c|}{d(1/T_f')} = \frac{d \ln t_\infty}{d(1/T_a)} \quad (7)$$

The values of $\Delta h/R$ determined from the cooling rate dependence of T_f' and the aging temperature dependence of t_∞ are 146.5 and 107.0 kK, respectively. Note that an average value of $\Delta h/R$=126.6 kK was used in the TNM modeling shown in Figures 2 and 3. The values of the apparent activation energy for polystyrene obtained in the current study lie on the high side of the range reported in Refs. [10,13,44–48] as shown in Table 2. The values of $\Delta h/R$ are comparable with those for Dylene 8 previously obtained in our laboratory [34,49]. We also note that the $\Delta h/R$ determined by the cooling rate

Table 2
The apparent activation energy $\Delta h/R$ for polystyrene

	M_n (g/mol)[a]	$\Delta h/R$ (kK)		Reference
		From cooling rate dependence of T_f' or T_g	From fit to the TNM or KAHR model[b]	
Enthalpy	15,700 (m)	77	–	[13]
	36,000 (m)	125[c]	–	[44]
	38,100 (m)	137	66	[45]
	68,000 (m)	129.6	–	[46]
	110,000 (m)	101.0	–	[47]
	200,000 (m)	–	176	[10]
	84,600	78.6	82.5	[10]
	92,800	–	100.4	[34]
		146.5, 107.0[d]	126.6[d]	This work
	198,000	78	–	[48]
Volume	92,800	125.6, 148.3	146.1	[34,49]

[a] m stands for monodispersed.
[b] The TNM model fit in this work and the fit to the volume relaxation data assumed an imperfect quench, whereas all the other model fits assumed perfect quenches.
[c] 80 kK without the data at 0.00172 K/min.
[d] 146.5 kK was obtained from the cooling rate dependence of fictive temperature, whereas 107.0 kK was obtained from the temperature dependence of the time required to reach equilibrium. An average value of 126.6 kK was used in the TNM modeling.

dependence of T_f' for polystyrene is higher than that determined by model fits to the enthalpy relaxation data as has been described previously [2,34,45]. However, some researchers have reported comparable values of $\Delta h/R$ determined from the curve fitting approach and from the cooling rate dependence of T_f' [10]. Hodge proposed that this discrepancy might be attributed to the thermal transfer effects [2]; however, this was shown not the case [50].

The Vogel [36] Tammann–Hesse [37] Fulcher [38] (VTHF) dependence of the time required to reach equilibrium versus aging temperature is depicted as the dashed line in Fig. 4 using parameters found earlier ($\log a_T = -12.8 + 370/(T - T_\infty)$, where $T_\infty = 69.8$ °C, $T_{ref} = T_\infty + 28.9$ °C) [34]. Although the temperature range investigated in this work is only 15 K, the aging temperature dependence of t_∞ and the cooling rate dependence of T_f' below T_g, especially at the lowest temperatures, both deviate from the WLF/VTHF temperature dependence and show no evidence for the existence of a critical temperature at which the relaxation time diverges. This behavior agrees with the result for polycarbonate reported by O'Connell and McKenna [51] and with our previous results for polystyrene [34] and selenium [52], as well as with the theoretical work of Di Marzio and Yang [53]. The data shown in Fig. 4 are also consistent with the assumed Arrhenius temperature dependence in the TNM/KAHR model. On the other hand, although WLF/VTHF temperature dependence has been observed below T_g by Schick et al., their experimental data only covers temperatures to 5 K below T_g [54,55].

3.2. Is the theoretical enthalpy limit achievable?

In order to determine the generality of our conclusion that the theoretical enthalpic liquid line is reached when the enthalpy stops evolving, we examined the dependence of equilibrium enthalpy loss on aging temperature for other polymers and small molecule glass formers using data reported in the literature. We examined aging data in which the enthalpy change had leveled off for at least three or more temperatures including data for polystyrene (PS) [56], polycarbonate (PC) [56,57], and polyetherimide (PEI) [58], as well as data for small molecule glass formers such as selenium (Se) [52] and triphenylethene (TPE) [56].

The enthalpy relaxation of polystyrene was investigated by Rault [56] after a quench at 50 K/min from above T_g. The enthalpy change observed at equilibrium is plotted in Fig. 5 as a function of aging temperature. The TNM model prediction for $\Delta H_{a\infty}$ (T_a) using an imperfect quench at a cooling rate of 50 K/min from 130 °C is shown as the solid line in Fig. 5 using the same set of TNM model parameters with ΔC_p of 0.265 J/g/K as were used for modeling our data. The model describes the data well and describes the breadth of the transition range similar to the results shown in Fig. 2. Note that the slope of the linear fit to the data at all aging temperatures yields a value of $-d\Delta H_{a\infty}/dT_a$ of 0.24 J/g/K, approximately 14% lower than the experimentally measured value of ΔC_p of 0.28 J/g/K (presumably measured on heating, which gives slightly larger values of ΔC_p than are observed on cooling [49]). As mentioned previously, the fact that data at the highest aging temperatures shows a slope considerably lower than the experimental value of ΔC_p is not due to aging not progressing to the theoretical liquid line as suggested by Cowie et al. [24–26], rather it is due to the breadth of the transition region.

The dependence of $\Delta H_{a\infty}$ on T_a for polycarbonate is shown in Fig. 6 for the data from Rault [56] and from Bauwens-Crowet and Bauwens [57]. The TNM model prediction, shown

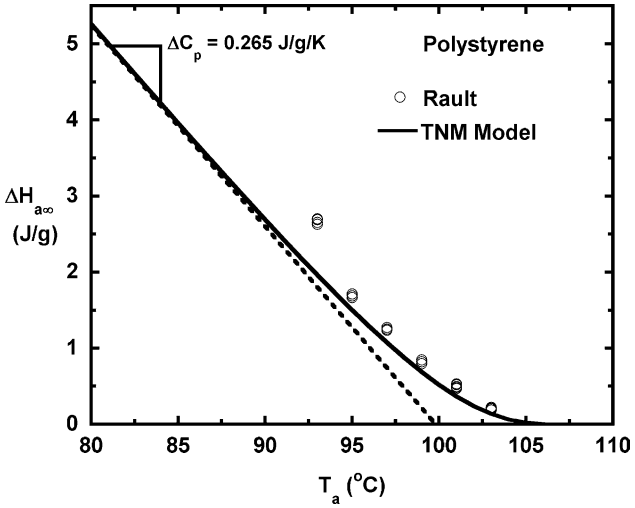

Fig. 5. Equilibrium enthalpy loss as a function of aging temperature for polystyrene reported by Rault [56]. The solid line shows the TNM model fit, and the dashed line shows a ΔC_p of 0.265 J/g/K and a T_{fo} of 99.8 °C.

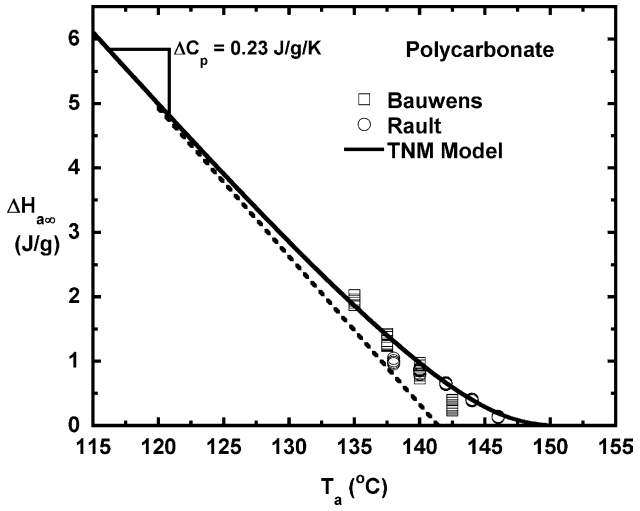

Fig. 6. Equilibrium enthalpy loss as a function of aging temperature for polycarbonate [56,57]. The solid line is the TNM model fit.

as the solid curve, was constructed using the parameters from the literature ($\Delta h/R = 150$ kK, $x = 0.19$, $\beta = 0.46$, $\ln(A/s) = -355.8$ [59], and $\Delta C_p = 0.23$ J/g/K [56]) and assuming a cooling rate of 30 K/min. The nominal cooling rates from Rault and Bauwens-Crowet and Bauwens' studies were reported to be 50 and 320 K/min, respectively; nevertheless, a reasonable description of the data is obtained assuming the literature values of the TNM parameters and a cooling rate of 30 K/min. Again, the fact that the slope of ΔH_∞ versus T_a is less than ΔC_p can be attributed the breadth of the glass transition and not due to failure to reach the liquid line at equilibrium.

The slopes of equilibrium enthalpy loss versus aging temperature for polyetherimide, selenium, and triphenylethene also show comparable or slightly lower values compared with the ΔC_p measured from DSC scans, as shown in Table 3, along with values for the polystyrene and polycarbonate studies already discussed. We suggest that the lower values of $-d\Delta H_{a\infty}/dT_a$ for selenium and triphenylethene also result from the breadth of glass transition region.

Table 3
The slopes for the equilibrium enthalpy loss versus aging temperature data, $-d\Delta H_{a\infty}/dT_a$, and ΔC_p measured from DSC scans

Material	Aging studies $-d\Delta H_{a\infty}/dT_a$ (J/g/K)	DSC scans ΔC_p (J/g/K)	Difference (%)	Reference
PS	0.26±0.01[a]	0.265	−1.9	This work, [34]
PS	0.24±0.02	0.28	−14	[56]
PC	0.21±0.01	0.23	−8.7	[57]
PC	0.11±0.01	0.23	−52	[56]
PEI	0.23±0.02	0.22	4.5	[58]
Se	0.12±0.01	0.13	−7.7	[52]
TPE	0.33±0.02	0.34	−2.9	[56]

[a] Data was obtained by linearly fitting the enthalpy loss data versus aging temperature below 98 °C.

4. Conclusions

Enthalpy relaxation of polystyrene was measured at temperatures ranging from the vicinity of glass transition temperature to 90 °C, 10 K below T_g, for aging times up to 200 days. Seven sets of enthalpy relaxation data were also re-examined for polymers and small molecule glass formers in the literature for cases where equilibrium was achieved at multiple temperatures. The slopes of the equilibrium enthalpy loss versus aging temperature, $-d\Delta H_{a\infty}/dT_a$, were compared with the ΔC_p measured by DSC scans. The lower values of the slopes, $-d\Delta H_{a\infty}/dT_a$, are attributed to the breadth of glass transition region, rather than being due to an inability to reach the theoretical enthalpy line as suggested by Cowie and Ferguson and others [24–26,29–31]. Our analysis backs up the arguments of Hutchinson and Kumar [19] regarding the importance of the breadth of the transition region on the temperature dependence of $\Delta H_{a\infty}$. Most importantly, our results indicate that the liquid enthalpy line is reached at temperatures below T_g when equilibrium is reached, i.e. when properties cease to evolve.

Acknowledgements

The authors would like to acknowledge American Chemical Society Petroleum Research Fund (grant number 39807-AC7) for their financial support to this project.

References

[1] Simon SL. In: Kroschwitz J, editor. Encyclopedia of polymer science and technology. New York: Wiley; 2003.
[2] Hodge IM. J Non-Cryst Solids 1994;169:211–66.
[3] McKenna GB. Comprehensive polymer science. In: Booth C, Price C, editors. Polymer properties, vol. 2. Oxford: Pergamon Press; 1989 [chapter 2].
[4] Plazek DJ, Berry GC. In: Uhlmann DRK, Kreidl NJ, editors. Glass: science and technology, vol. 3. New York: Academic Press, Inc.; 1986.
[5] Kovacs AJ, Aklonis JJ, Hutchinson JM, Ramos AR. J Polym Sci B: Polym Phys 1979;17:1097–162.
[6] Tool AQ. J Am Ceram Soc 1946;29:240–53.
[7] Narayanaswamy OS. J Am Ceram Soc 1971;54:491–8.
[8] Moynihan CT, Macedo PB, Montrose CJ, Gupta PK, DeBolt MA, Dill JF, et al. Ann NY Acad Sci 1976;279:15–35.
[9] Ngai KL. Comments Solid State Phys 1979;9:127–40.
[10] Hodge IM, Huvard GS. Macromolecules 1983;16:371–5.
[11] Scherer GW. J Am Ceram Soc 1986;69:374–81.
[12] Tribone JJ, O'Reilly JM, Greener J. J Polym Sci B: Polym Phys 1989;27:837–57.
[13] O'Reilly JM, Hodge IM. J Non-Cryst Solids 1991;131–133:451–6.
[14] Rekhson S, Ducroux J-P. In: Pye LD, La Course WC, Stevens HJ. editors. The Physics of non-crystalline solids. London: Taylor Francis; 1992, p. 315.
[15] Moynihan CT, Crichton SN, Opalka SM. J Non-Cryst Solids 1991;131–133:420–34.
[16] Moynihan CT. Rev Miner 1995;32:1–19.
[17] Medvedev G, Caruthers JM. In Proceedings of the the society of rheology 71st annual meeting. Madison, WI, October 17–21 1999. Paper SL7.
[18] Simon SL, Bernazzani P. J Non-Cryst Solids, in press.
[19] Hutchinson JM, Kumar P. Thermochim Acta 2002;391:197–217.
[20] Kovacs AJ. PhD Thesis. University of Paris, 1954.
[21] Fujimori H, Fujita H, Oguni M. Bull Chem Soc Jpn 1995;68:447–55.

[22] Yamamuro O, Takahara S, Suga H. J Non-Cryst Solids 1995;183:144–50.
[23] Takahara S, Yamamuro O, Ishikawa M, Matsuo T, Suga H. Rev Sci Instrum 1998;69:185–92.
[24] Cowie JMG, Ferguson R. Polymer 1993;34:2135–41.
[25] Cowie JMG, Harris S, McEwen IJ. J Polym Sci B: Polym Phys 1997;35: 1107–16.
[26] Cameron NR, Cowie JMG, Ferguson R, McEwan I. Polymer 2000;41: 7255–62.
[27] Williams G, Watts DC. Trans Faraday Soc 1970;66:80–5.
[28] Kolrausch F. Pogg Ann Phys 1847;12:393.
[29] Gómez Ribelles JL, Monleón Pradas M. Macromolecules 1995;28: 5867–77.
[30] Gómez Ribelles JL, Monleón Pradas M, Vidaurre Garayo A, Romero Colomer F, Más Estellés J, Meseguer Dueñas JM. Macromolecules 1995; 28:5878–85.
[31] Gómez Ribelles JL, Monleón Pradas M, Vidaurre Garayo A, Romero Colomer F, Más Estellés J, Meseguer Dueñas JM. Polymer 1997;38: 963–9.
[32] Colby RH. Phys Rev E 2000;61:1783–92.
[33] Boltzmann L. Wied Ann 1878;5:430.
[34] Simon SL, Sobieski JW, Plazek DJ. Polymer 2001;42:2555–67.
[35] Williams ML, Landell RF, Ferry JD. J Am Chem Soc 1955;77:3701–7.
[36] Vogel H. Phys Z 1921;22:645–6.
[37] Tammann G, Hesse G. Z Anorg Allg Chem 1926;156:245–7.
[38] Fulcher GS. J Am Chem Soc 1925;8:339–55 see also p. 789–794.
[39] Petrie SEB. J Polym Sci A-2 1972;10:1255–72.
[40] Debolt MA, Easteal AJ, Macedo PB, Moynihan CT. J Am Ceram Soc 1976;59:16–21.
[41] Moynihan CT, Easteal AJ, Wilder J. J Phys Chem 1974;78:2673–7.
[42] Sobieski JW. PhD Thesis. University of Pittsburgh, 1999.
[43] Kuester JL, Mize JH. Optimization techniques with Fortran. New York: McGraw-Hill; 1973.
[44] Stevens GC, Richardson MJ. Polym Commun 1985;26:77–80.
[45] Prest Jr. WM, Roberts FJ, Hodge IM. In: Proceedings of the 12th NATAS conference. Virginia: Williamsburg; 1982. p. 119–23.
[46] Aras L, Richardson MJ. Polymer 1989;30:2246–52.
[47] Privalko VP, Demchenko SS, Lipatov YS. Macromolecules 1986;19: 901–4.
[48] Wunderlich B, Bodily DM, Kaplan MH. J Appl Phys 1964;35:95–102.
[49] Badrinarayanan P, Zheng W, Li Q, Simon SL. To be submitted for publication.
[50] Simon SL. Macromolecules 1997;30:4056–63.
[51] O'Connell PA, McKenna GB. J Chem Phys 1999;10:11054–60.
[52] Echeverria I, Kolek PL, Plazek DJ, Simon SL. J Non-Cryst Solids 2003; 324:242–55.
[53] Di Marzio EA, Yang AJM. J Res Nat Inst Stand Technol 1997;102: 135–57.
[54] Weyer S, Merzlyakov M, Schick C. Thermochim Acta 2001;377: 85–96.
[55] Weyer S, Huth H, Schick C. Polymer 2005;46:12240–6.
[56] Rault J. J Phys: Condens Matter 2003;15:S1193–S213.
[57] Bauwens-Crowet C, Bauwens J-C. Polymer 1986;27:709–13.
[58] Echeverria I, Su PC, Simon SL, Plazek DJ. J Polym Sci B: Polym Phys 1995;33:2457–68.
[59] Hodge IM. Macromolecules 1987;20:2897–908.